Study of the process $e^+e^- \to \pi^+\pi^-\pi^0\eta$ at the SND detector

Alexander Botov[1,⋆]

[1] *Budker Institute of Nuclear Physics, Novosibirsk, 630090, Russia*

Abstract. The reaction $e^+e^- \to \pi^+\pi^-\pi^0\eta$ has been studied in the center-of-mass energy region below 2 GeV in the experiment with the SND detector at the VEPP-2000 e^+e^- collider. The reaction proceeds via the four intermediate states: $\omega\eta$, $\phi\eta$, $a_0(980)\rho$, and a structureless $\pi^+\pi^-\pi^0\eta$ state, which may be, for example, $\rho(1450)\pi$ state with $\rho(1450) \to \rho(770)\eta$. The total $e^+e^- \to \pi^+\pi^-\pi^0\eta$ cross section and the cross section for its components, $\omega\eta$, $\phi\eta$, and a sum of $a_0(980)\rho$ and the structureless state, have been measured separately. Our results are in agreement with previous measurements and have comparable or better accuracies.

1 Introduction

The main goal of experiments at the VEPP-2000 e^+e^- collider [1] is the precision measurement of the total cross section of e^+e^- annihilation into hadrons in the center-of-mass (c.m.) energy (E) region below 2 GeV. The total cross section is necessary for calculation of the running electromagnetic coupling constant and the muon anomalous magnetic moment. Below 2 GeV the total hadronic cross section is determined as a sum of exclusive cross sections for all possible hadronic channels. The process $e^+e^- \to \pi^+\pi^-\pi^0\eta$ gives a sizeable contribution to the total cross section above 1.6 GeV. It was established [2] that the $e^+e^- \to \pi^+\pi^-\pi^0\eta$ reaction proceeds through $\omega\eta$, $\phi\eta$, $a_0(980)\rho$ intermediate states and a structureless $\pi^+\pi^-\pi^0\eta$ mechanism ($nres$). The latter may be, for example, $\rho(1450)\pi$ state with $\rho(1450) \to \rho(770)\eta$ decay. The cross sections for $e^+e^- \to \omega\eta$ and $\phi\eta$ were previously measured in several final states [3–9]. The only measurement of the $e^+e^- \to \pi^+\pi^-\pi^0\eta$ reaction and the cross sections for the subprocesses $e^+e^- \to a_0\rho$ and $e^+e^- \to nres$ was performed in the CMD-3 experiment [9] also at VEPP-2000.

This work is dedicated to the measurement of the $e^+e^- \to \pi^+\pi^-\pi^0\eta$ cross section at the SND detector [10]. We analyze the $\pi^+\pi^-\pi^0\eta$ final state with the η meson decayed to $\gamma\gamma$ and measure separately cross section for its intermediate states.

2 Data and simulation

This analysis is based on data with an integrated luminosity of 27 pb^{-1} recorded with the SND detector in 2011–2012 in 36 energy points of the range 1.34–2 GeV, that is above the threshold of the process under study. Experimental energy points are merged into 13 energy intervals with 50 MeV width.

⋆e-mail: A.A.Botov@inp.nsk.su

Simulation of the signal and background processes is done with Monte Carlo (MC) event generators. The generators take into account radiative corrections to the initial particles calculated according to Ref. [11]. The energy dependencies of Born cross sections needed for calculations of the radiative corrections are obtained from data using an iterative procedure. As a first approximation we take the cross sections from Ref. [4] for the $\omega\eta$, from Ref. [5] for the $\phi\eta$, and from Ref. [9] for the $a_0\rho$, $nres$ intermediate states. For the total $e^+e^- \to \pi^+\pi^-\pi^0\eta$ process the initial Born cross section is taken from Ref. [2]. To determine the energy dependence of the detection efficiency for the last process and for the sum of the $a_0\rho$ and $nres$ intermediate states simulation in the $e^+e^- \to \rho(1450)\pi$, $\rho(1450) \to \rho\eta$ model is used.

The luminosity is measured using the process of Bhabha scattering $e^+e^- \to e^+e^-$ with the systematic uncertainty less than 1%.

3 Event selection

The following preselection is used. There are two or three charged particles originated from the interaction region and at least four photons with energy greater than 20 MeV in an event. The total energy deposition in the calorimeter for these events is required to be greater than 300 MeV.

For preliminary selected events the vertex fit characterized by the parameter χ^2_r is performed using the parameters of two charged tracks. If there are three charged tracks in an event, the two tracks with the lowest χ^2_r value are selected. The found vertex is used to redefine the measured angles of charged particles and photons. Then a kinematic fit to the $e^+e^- \to \pi^+\pi^-\pi^0\gamma\gamma$ hypothesis characterized by the parameter $\chi^2_{3\pi2\gamma}$ is performed with the requirement of energy and momentum balance and the invariant mass of the π^0 candidate constrained to its world average value [12]. The fit uses the measured polar and azimuthal angles of charged particles, and the measured angles and energies of photons. The invariant mass of the photon pair, which is assumed to be the η-meson candidate, must be in the range $400 < M_{\gamma\gamma} < 700$ MeV. All possible combinations of photons are tested and the combination with the smallest $\chi^2_{3\pi2\gamma}$ is chosen. The photon parameters after the kinematic fit are used to recalculate the η-candidate invariant mass (M_η). The event is then refitted with the η-mass constraint. The refined η-candidate energy is used to calculate the invariant mass of the system recoiling against the η meson (M^{rec}_η).

Events of the process under study are selected by the condition $\chi^2_{3\pi2\gamma} < 30$. To suppress background from the process $e^+e^- \to \pi^+\pi^-\pi^0\pi^0$ we perform a kinematic fit to the hypothesis $e^+e^- \to \pi^+\pi^-\pi^0\pi^0(\gamma)$ (radiation of an additional photon along the beam axis is allowed) and reject events with $\chi^2_{4\pi(\gamma)} < 200$.

4 Determination of the number of signal events

The M_η spectrum for selected data events is shown in Fig. 1. To extract the number of signal $e^+e^- \to \pi^+\pi^-\pi^0\eta$ events the spectrum is fitted with a sum of signal and background distributions in each energy interval. The background distribution is a sum of the simulated distribution for $e^+e^- \to \pi^+\pi^-\pi^0\pi^0$ and a linear function. The signal distribution is described by a sum of three Gaussian distributions with parameters determined from the fit to the simulated M_η distribution for $e^+e^- \to \pi^+\pi^-\pi^0\eta$ events.

The total distribution of the signal events for invariant mass M^{rec}_η is shown in Fig. 2. The number of events in each M^{rec}_η bin is determined from the fit to the M_η distribution as described above. The ω- and ϕ-meson peaks are clearly seen. We define contributions of the intermediate states through approximation of these spectra constructed for each energy interval with a sum of simulated distributions for them. For $\omega\eta$ and $\phi\eta$ channels we use three Gaussian distributions with parameters determined

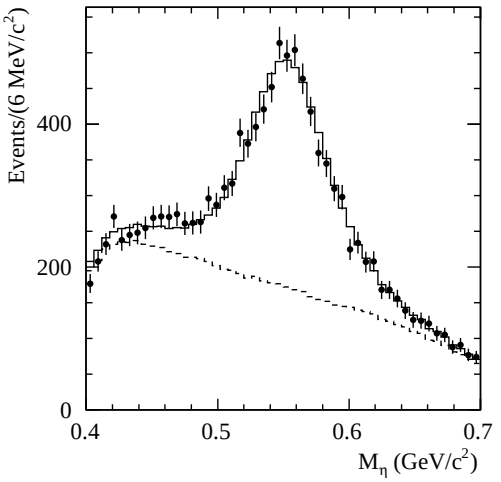

Figure 1. The M_η spectrum for selected data events (points with error bars). The solid histogram is the result of the fit to the data spectrum with a sum of signal and background distributions. The fitted background contribution is shown by the dashed histogram.

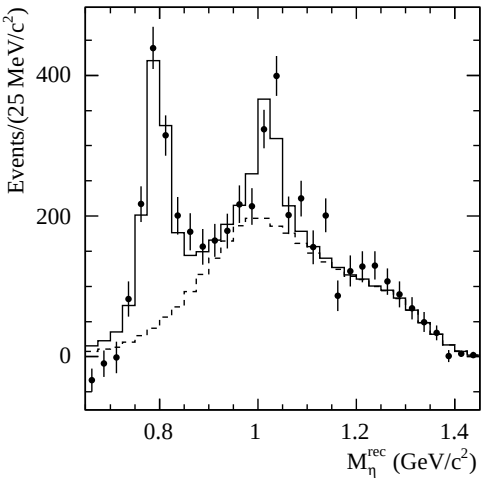

Figure 2. The M_η^{rec} distribution for data $e^+e^- \to \pi^+\pi^-\pi^0\eta$ events (points with error bars). The solid histogram represents the result of the fit described in the text. The dashed histogram represents the sum of the $e^+e^- \to a_0\rho$ and $e^+e^- \to nres$ contributions.

from the fit to the simulated distributions. For the $a_0\rho$ and structureless $e^+e^- \to \pi^+\pi^-\pi^0\eta$ decay channels simulated histograms are used. These histograms are wide and have similar shapes. Therefore, in the further analysis we do not separate these two mechanisms. The ratio for them is fixed at the value measured in Ref. [9] and is allowed to vary within its uncertainty during the fit.

5 The Born cross section

The experimental values of the each visible cross section are calculated as follows,

$$\sigma_{vis,i} = \frac{N_i}{L_i \varepsilon_i B}, \tag{1}$$

where N_i, L_i, and ε_i are the number of selected data events, integrated luminosity, and detection efficiency for the i-th energy interval, and B is the branching fraction of decay to the $\pi^+\pi^-\pi^0\eta$ final state which for the $\omega\eta$ and $\phi\eta$ channels is taken from Particle Data Group (PDG) [12] and for the rest two is equal to unit.

Experimental values of the Born cross section are determined as follows, $\sigma_i = \sigma_{vis,i}/(1 + \delta(\overline{E}_i))$, where $\delta(\overline{E}_i)$ is the radiative correction, calculated from the fit to $\sigma_{vis,i}$ with theoretical model of the Born cross section as described in Ref. [4].

The two-resonance model is used to parametrize the Born cross sections

$$\sigma(E) = \frac{12\pi}{E^3}\left|\sqrt{\frac{B_{V'}}{P_f(m_{V'})}}\frac{m_{V'}^{3/2}\Gamma_{V'}}{D_{V'}} + \sqrt{\frac{B_{V''}}{P_f(m_{V''})}}\frac{m_{V''}^{3/2}\Gamma_{V''}}{D_{V''}}e^{i\varphi}\right|^2 P_f(E), \tag{2}$$

where m_V and Γ_V are the mass and width of the resonance V ($V = V'$ or V''), $D_V = E^2 - m_V^2 + iE\Gamma_V$, $B_V = B(V \to e^+e^-)B(V \to f)$ is the product of the branching fractions for the V decay to e^+e^- and the final state f, and $P_f(E)$ is the phase space factor.

For the $\omega\eta$ channel the first term in Eq. (2) is associated with the $\omega(1420)$ resonance, the second is a sum of contributions of the $\omega(1650)$ and $\phi(1680)$ resonances, and $P_f(E) = q_\omega^3(E)$, where $q_\omega(E)$ is the ω momentum in the reaction $e^+e^- \to \omega\eta$. The phase between the first and second terms in Eq. (2) is chosen to be equal to π [4]. In the fit to the $e^+e^- \to \omega\eta$ cross-section data the free parameters are $B_{V'}$, $B_{V''}$, $m_{V''}$, and $\Gamma_{V''}$. The V' mass and width are fixed at the Particle Data Group (PDG) values for $\omega(1420)$ [12].

For the $\phi\eta$ channel we use one resonance model with $B_{V'} = 0$ and $P_f(E) = q_\phi^3(E)$, where $q_\phi(E)$ is the ϕ momentum in the reaction $e^+e^- \to \phi\eta$. The obtained V'' mass and width are in agreement with the PDG values for the $\phi(1680)$.

The $e^+e^- \to a_0\rho + nres \to \pi^+\pi^-\pi^0\eta$ and $e^+e^- \to \pi^+\pi^-\pi^0\eta$ cross sections are described by the model (2) with seven free parameters ($B_{V'}$, $m_{V'}$, $\Gamma_{V'}$, $B_{V''}$, $m_{V''}$, $\Gamma_{V''}$, and φ) and $P_f(E) = q_\omega(E)$. This model describes data well, and therefore can be used to calculate radiative corrections.

The fitted curves together with obtained values of the Born cross sections are shown in Fig. 3. The obtained $e^+e^- \to \omega\eta$ cross section agrees with the CMD-3 measurement [9]. Both the SND and CMD-3 results lie below the *BABAR* data [3]. The SND and *BABAR* [5] measurements of the $e^+e^- \to \phi\eta$ cross sections are in reasonable agreement. The considerable difference between the SND and CMD-3 measurements is observed for the $e^+e^- \to a_0\rho + nres$ cross sections. The total $e^+e^- \to \pi^+\pi^-\pi^0\eta$ cross section measured by SND is, in general, consistent with the CMD-3 result [9]. The $\sim 15\%$ difference in the cross section maximum is within the systematic uncertainties, which are 7% for SND and 11% for CMD-3.

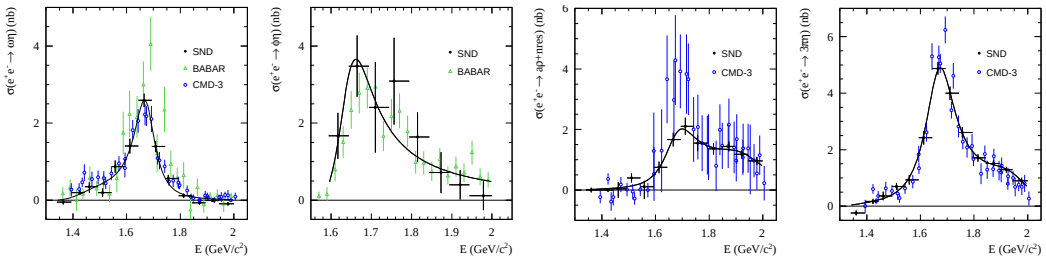

Figure 3. The cross sections for processes with intermediate states $\omega\eta$, $\phi\eta$, $a_0\rho + nres$ and for the total process $e^+e^- \to \pi^+\pi^-\pi^0\eta$ measured in this work (filled circles) and in the previous experiments [3, 6, 9] (open circles and triangles). Only statistical errors are drawn. The curves are the results of the fit described in the text.

6 Conclusions

In this paper we present the analysis of the process $e^+e^- \to \pi^+\pi^-\pi^0\eta$ from the SND detector at the VEPP-2000 e^+e^- collider. We have measured the cross section for this process and for its subprocesses $e^+e^- \to \omega\eta$, $e^+e^- \to \phi\eta$ and $e^+e^- \to a_0\rho + nres$, where $nres$ is the structureless $\pi^+\pi^-\pi^0\eta$ state, in the c.m. energy range 1.34–2.00 GeV. The cross sections have a peak near the energy $\simeq$ 1650 MeV. The obtained cross sections are rather consistent with the previous experiments and have comparable or better accuracy. The obtained $e^+e^- \to \omega\eta$ and $e^+e^- \to \phi\eta$ cross sections are well fitted in the VMD model with the $\omega(1420)$, $\omega(1650)$ and $\phi(1680)$ resonances.

References

[1] A. Romanov *et al.*, in *Proceedings of Particle Accelerator Conference PAC 2013*, Pasadena, CA USA, p. 14, (2013).

[2] V. P. Druzhinin *et al.* (*SND* Collaboration), EPJ Web Conf. **130**, 05004 (2016) [arXiv:1609.01040 [hep-ex]].

[3] B. Aubert *et al.* (*BABAR* Collaboration), Phys. Rev. D **73**, 052003 (2006).

[4] M. N. Achasov *et al.* (*SND* Collaboration), Phys. Rev. D **94**, 092002 (2016).

[5] B. Aubert *et al.* (*BABAR* Collaboration), Phys. Rev. D **76**, 092005 (2007).

[6] B. Aubert *et al.* (*BABAR* Collaboration), Phys. Rev. D **77**, 092002 (2008).

[7] J. P. Lees *et al.* (*BABAR* Collaboration), Phys. Rev. D **95**, 052001 (2017).

[8] M. N. Achasov *et al.* (*SND* collaboration), Phys. Atom. Nucl. **81**, 205 (2018) [Yad. Fiz. **81**, no. 2, 195 (2018)].

[9] R. R. Akhmetshin *et al.* (*CMD-3* Collaboration), Phys. Lett. B **773**, 150 (2017).

[10] M. N. Achasov *et al.*, Nucl. Instrum. Methods Phys. Res., Sect. A **598**, 31 (2009); V. M. Aulchenko *et al.*, *ibid.* **598**, 102 (2009); A. Yu. Barnyakov *et al.*, *ibid.* **598**, 163 (2009); V. M. Aulchenko *et al.*, *ibid.* **598**, 340 (2009).

[11] E. A. Kuraev and V. S. Fadin, Yad. Fiz. **41**, 733 (1985) [Sov. J. Nucl. Phys. **41**, 466 (1985)].

[12] K. A. Olive *et al.* (Particle Data Group), Chin. Phys. C **38**, 090001 (2014).